J. Phys.: Condens. Matter 6 (1994) 5423–5437. Printed in the UK

Conductance behaviour near the metal–insulator transition on a disordered Bethe lattice

P M Bell and A MacKinnon

Condensed Matter Theory Group, The Blackett Laboratory, Imperial College, Prince Consort Road, London SW7 2BZ, UK

Received 14 March 1994, in final form 15 April 1994

Abstract. Using a model of random one-dimensional wires, we determine an exact recursive formula for the transmission probability of a Bethe lattice. We use this formula, in numerical simulations, to study the metal–insulator transition. In particular, we examine the form of the conductance distribution and find that it does not obey the predictions given in other studies.

1. Introduction

In a previous paper [1], we calculated the critical exponents of the Anderson metal–insulator transition [2, 3] on a network of random wires. The exponents of the transition are an important quantity and, as was detailed in that paper, there is still doubt over the actual values of these exponents [1, 4, 5]. However, in order to study the nature of the Anderson transition itself, perhaps the most important quantity to study is the conductance distribution. In particular, is it possible to identify any characteristic behaviour in the conductance distribution as the system being studied is driven from the metallic to the insulating regime? Above all, what happens to the conductance distribution at, and near, the transition point? Detailed theoretical work has been done mainly in one dimension [6, 7, 8, 9] and only limited theoretical and numerical work exists in higher dimensions [10, 11, 12], due to the immense technical difficulties involved.

Because of these difficulties, approximations have to be made. One such approximation is to study the conductance on a Bethe lattice [13]. The Bethe lattice can be characterized by its connectivity K which is just equal to one less than the number of nearest neighbours Z. That is, $K = Z - 1$. The Bethe lattice has no closed paths and the number of sites on its surface are as numerous as the number inside. An example of a Bethe lattice with connectivity $K = 2$ is shown in figure 1. The numbers by the lattice sites indicate the shell of the Bethe lattice, n. So the number of sites, N, in a particular shell is $N = K^n$. Another property, due to the lack of any ring structures, is that any two points on the lattice are connected by only one, unique, path. This absence of ring structures makes theoretical studies tractable but prohibits any weak-localization effects and, therefore, the Bethe lattice can only serve as an approximation to a real lattice for studying the metal–insulator transition. The Bethe lattice is believed to represent a space of infinite dimensionality and, therefore, any transition on such a lattice must represent only a mean-field approximation.

The Bethe lattice was first studied, with reference to the Anderson transition, by Abou-Chacra *et al* in 1973 [14]. They derived an equation for the self-energy which could be solved self-consistently, but which was exact on a Bethe lattice. From this they proved the existence of localized states at certain disorders and achieved an estimate of the mobility

0953-8984/94/285423+15$19.50

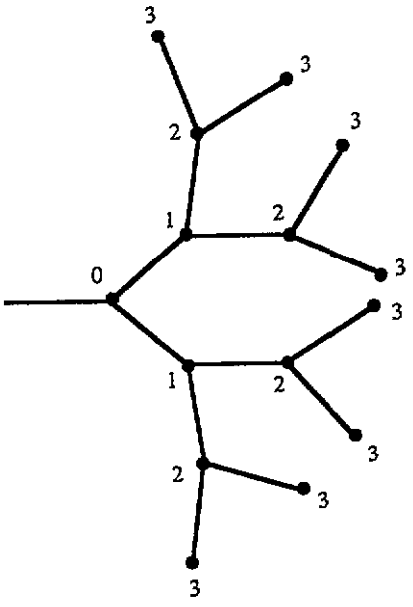

Figure 1. A Bethe lattice of connectivity $K = 2$. This figure shows only the first four shells of the lattice.

edges. They did not, however, prove that truly extended states exist outside the localized energy-disorder regions, nor did they analyse the neighbourhood of the transition. These points were given more thorough investigation by Kunz and Souillard in 1983 [15], when they showed that a transition from extended to localized wavefunctions did occur on the Bethe lattice when the disorder or energy were varied. They claimed their model was the first to show the definite existence of an Anderson transition. They also obtained an exponent for the divergence of the localization length of $\nu = 1$.

Shapiro [16] also studied the Bethe lattice, using a model of channels and beam splitters. The model defined in this paper is similar to Shapiro's, in the sense that both make use of the scattering matrix formalism. By finding an equation for the reflection of the lattice, Shapiro found the existence of a continuous MIT and a value for the conductivity exponent of $t = 1$, using an analytic approach.

Most recently, Chalker and Siak [17] studied the Anderson Hamiltonian on a Bethe lattice. They found, as expected, a transition between extended eigenstates at weak scattering and exponentially localized eigenstates at strong scattering. However, they also emphasized that on a Bethe lattice three phases and two transitions exist; the less obvious transition being from a power-law-decaying wavefunction to an exponentially decaying wavefunction, but with both wavefunctions giving rise to conduction. This is due, principally, to the strange geometry of the Bethe lattice, which makes the conditions for normalization of the wavefunctions different from that on a 'normal' lattice.

In all these references, it is a criterion for localization which has been sought, hence the search for critical disorders or energy. Also, in two of the references the exponents were determined, the nature of the Bethe lattice making these calculations tractable. In this paper we extend the work of these authors: we study the Bethe lattice numerically for the existence of a transition, then we examine the behaviour of the conductance distribution around this critical point.

2. The model

Consider some initial distribution of random one-dimensional wires. These wires can be completely described by their scattering matrix **S**, figure 2. The amplitudes of the input and output waves are related by the scattering matrix in the following way:

$$\begin{pmatrix} B \\ C \end{pmatrix} = \mathbf{S} \begin{pmatrix} A \\ D \end{pmatrix} \tag{1}$$

where

$$\mathbf{S} = \begin{pmatrix} |r|e^{i\theta_r} & |t|e^{i\theta_t} \\ |t|e^{i\theta_t} & |r|e^{i(2\theta_t - \theta_r + \pi)} \end{pmatrix} \tag{2}$$

and $|r|, |t|$ are the reflection and transmission amplitudes respectively and θ_r, θ_t are the reflection and transmission phases. This scattering matrix describes a one-dimensional wire in the absence of a magnetic field and with no spin–orbit coupling.

Figure 2. The input and output amplitudes from a one-dimensional disordered wire, which are related by the scattering matrix.

Now, to construct a Bethe lattice of connectivity K, we randomly select K wires from the distribution. These K wires must then be joined at a single node. In order to perform this operation, we attach these K wires to an infinitesimally small piece of perfect wire; that is, a piece of wire which is perfectly transmitting. Stage 1 of figure 3 shows this procedure. In a previous paper [1], we explained the conditions which must be satisfied at a node where several one-dimensional wires are joined. Namely, the amplitude of the waves on each of the wires must be the same at the node and the sum of the first derivatives must be zero (taking care of the direction) at that node.

A wave on the ith wire, starting at the node and moving along the wire, will have an amplitude

$$\psi_i = A_i(1 + r_i) \tag{3}$$

at the node, because the amplitude of the reverse travelling part of the wave is given by the product of the forward-travelling amplitude A_i and the reflection coefficient r_i of the wire. The amplitude of the wave on the perfect infinitesimally small wire will be

$$\psi_{K+1} = A_{K+1}(1 + r') \tag{4}$$

where r' is the new reflection of the junction. Thus the condition of equal amplitudes gives

$$\psi_1 = \psi_2 = \ldots = \psi_{K+1} \tag{5}$$

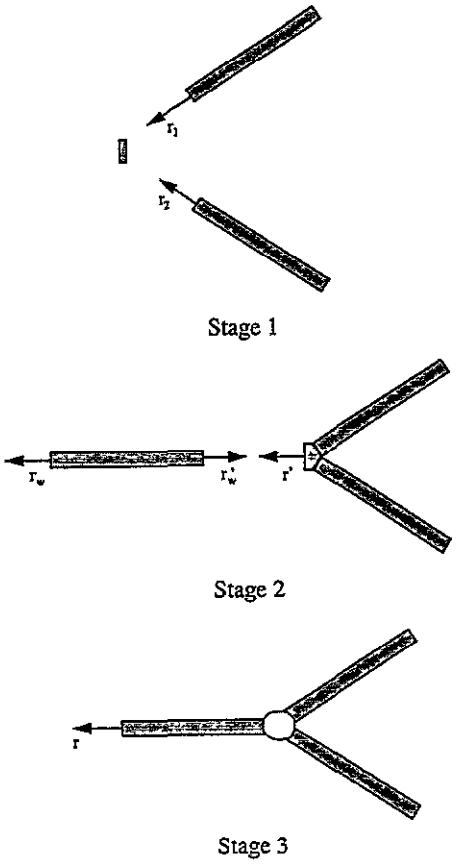

Figure 3. The first three stages needed to form a Bethe lattice with connectivity $K = 2$. stage 1 of the recursive procedure is to join two random wires to an infinitesimally small piece of perfect wire. At stage 2, another random wire is attached to the junction formed by stage 1. Stage 3 shows the new system with reflection r from the end.

or

$$A_1(1 + r_1) = A_2(1 + r_2) = \ldots = A_{K+1}(1 + r'). \tag{6}$$

The current-conservation (first-derivative sum) condition gives

$$A_1(1 - r_1) + A_2(1 - r_2) + \ldots = A_{K+1}(1 - r') \tag{7}$$

noting that the direction of the derivative has been reversed for the wave on the infinitesimal wire. Again, using the same arguments as in [1], the value of the wavenumber is assumed to be the same for all waves at the node. The above equation can be written more succinctly as

$$A_{K+1}(1 - r') = \sum_{i=1}^{K} A_i(1 - r_i). \tag{8}$$

Dividing the LHS of this equation by the amplitude of the $(K+1)$th wave at the node gives

$$\frac{(1-r')}{(1+r')} = \frac{1}{A_{K+1}(1+r')} \sum_{i=1}^{K} A_i(1-r_i). \tag{9}$$

But, from the amplitude condition (6),

$$A_{K+1}(1+r') = A_i(1+r_i) \qquad \forall i \in (1, K). \tag{10}$$

Therefore

$$\frac{(1-r')}{(1+r')} = \sum_{i=1}^{K} \frac{(1-r_i)}{(1+r_i)}. \tag{11}$$

The reflection from the junction, formed by joining K wires together, is

$$r' = \left(1 - \sum_{i=1}^{K} \frac{(1-r_i)}{(1+r_i)}\right) \Bigg/ \left(1 + \sum_{i=1}^{K} \frac{(1-r_i)}{(1+r_i)}\right). \tag{12}$$

In order to go from stage 2 to stage 3 of figure 3, another one-dimensional wire must be attached to the newly formed junction. The new reflection from this object, r, will involve two terms: a simple reflection from the end of the one-dimensional wire and a multiple-scattering term due to reflections from the opposite end of the wire and the junction. Including both these terms gives an expression for the reflection r of the system shown in stage 3 of figure 3 of

$$r = r_w + t_w r' t_w \sum_{n=0}^{\infty} (r'_w r')^n \tag{13}$$

and since $|r'_w|$ and $|r|$ must be less than unity,

$$r = r_w + \frac{t_w r' t_w}{1 - r'_w r'} \tag{14}$$

where t_w is the transmission coefficient of wire 3, r_w and r'_w are the reflection coefficients from the left- and right-hand side of wire 3 respectively and r' is the reflection of the junction, equation (12). Thus, we have determined the reflection from the end of a Bethe lattice of size one shell.

However, examination of the procedure just detailed shows that it can be repeated using Bethe lattice sections of arbitrary shell number and a single one-dimensional wire, since it is only required to know the reflection from the end of the objects being joined. Therefore, it is clear that stages 1, 2 and 3 of figure 3 show an exact recursive procedure for generating very large Bethe lattices. The procedure is successful for the Bethe lattice, since any arbitrarily sized Bethe lattice section can be characterized by the reflection from its end (or centre) and can therefore replace the one-dimensional wires with reflections r_1 and r_2 in stage 1 of figure 3.

So we can calculate the transmission probability (and hence the conductance) of a very large Bethe lattice by repeatedly using the above recursive procedure (equations (12) and

(14)) and then applying the current-conservation condition $|t|^2 = 1 - |r|^2$, where r is the calculated reflection coefficient for that Bethe lattice. The conductance is then trivially obtained from the Landauer formula, $G = (e^2/(2\pi\hbar))|t|^2$ [18].

Unfortunately, this procedure proves to be numerically unstable when the reflection coefficient of the lattice becomes close to unity. Since a reflection coefficient of unity signals the insulating regime, this means that the instability occurs in the region of the metal–insulator transition, precisely where we wish to perform our calculations! Therefore, we need to find an alternative formulation of the recursive procedure which will give us the transmission probability without relying so explicitly on the reflection probability: notice that we have to subtract two almost equal numbers which will obviously result in a loss of accuracy (irrespective of whether r is unstable or not).

Consider again the argument we used for joining K branches together at a single node by attaching them to a small piece of perfectly transmitting one-dimensional wire (see stage 1 of figure 3). Let each of the branches have reflection r_i from the end and a transmission coefficient t_i. Let A_i be the amplitude of the wave starting at the end of the branch, nearest the node, and travelling along it. Then the amplitude of the wave transmitted through the ith branch is

$$t_i A_i.$$

Now, let $|i\rangle$ represent the ith branch, through which current is being transmitted. At the surface of the lattice, the waves do not interfere since they are spatially separated from one another. Hence the $|i\rangle$ must obey

$$|i\rangle\langle j| = \delta_{ij} \tag{15}$$

and the total amplitude of all waves, α, transmitted through the joined branches will be just

$$\alpha = \sum_{i=1}^{K} t_i A_i |i\rangle. \tag{16}$$

If a wave with amplitude A_{K+1} is fed into the junction formed by joining the K branches to the perfect small wire, then the total transmitted current is just

$$|A_{K+1}|^2|t'|^2 = |\alpha|^2 \tag{17}$$

where $|t'|^2$ is the transmission probability of the junction. Therefore,

$$|A_{K+1}|^2|t'|^2 = \left|\sum_{i=1}^{K} t_i A_i |i\rangle\right|^2 \tag{18}$$

or

$$|t'|^2 = \frac{1}{|A_{K+1}|^2} \sum_{i=1}^{K} |A_i|^2 |t_i|^2 \tag{19}$$

because there is no interference between waves at the surface. Now, equation (10) can be written in the form

$$\frac{A_i}{A_{K+1}} = \frac{1 + r'}{1 + r_i} \tag{20}$$

where r' is the reflection of the junction. Hence

$$|t'|^2 = |1 + r'|^2 \sum_{i=1}^{K} \frac{|t_i|^2}{|1 + r_i|^2}. \tag{21}$$

With this expression, we have determined the transmission probability of the junction formed by joining K wires together at a single node. But in order for us to form a Bethe lattice, a one-dimensional wire must be attached to the junction. Let the wire have transmission coefficient t_w and a reflection from its RHS of r'_w. Then the transmission probability through the Bethe lattice section $|t|^2$, formed by joining the RHS of the wire to the junction will be

$$|t|^2 = |t_w|^2 \frac{|1 + r'|^2}{|1 - r_w r'|^2} \sum_{i=1}^{K} \frac{|t_i|^2}{|1 + r_i|^2}. \tag{22}$$

This expression can be used recursively, in conjunction with equation (12), to determine the transmission probability of the Bethe lattice as it grows in size. Notice that we still require to calculate the reflection from the junction and use it in the expression for the transmission probability. However, we have altered its rôle in the calculation of the transmission and thus hopefully increased the stability of the procedure for calculating the transmission probability. Also note that we have removed the potentially accuracy-limiting step of subtracting two almost equal numbers. Extensive numerical tests on both methods indicated to us that this was indeed the case and for the remainder of this paper, we calculate the transmission probabilities of the growing Bethe lattice using equations (12) and (22).

3. Algorithm

The equations (12) and (22), which define the exact recursive procedure for calculating the transmission probabilities of arbitrarily large Bethe lattices, are useful for two reasons: the equations are simple and therefore ideally suited to numerical computation, and by storing the relevant variables of a large number of Bethe lattice sections at each step, quantities such as the transmission probability (and thus the conductance) distribution can be studied.

We set up the numerical simulation of a disordered Bethe lattice as follows: define an initial array of N disordered one-dimensional wires, forming the distribution of transmission probabilities. For the surface of the Bethe lattice we need to choose some boundary conditions. In this case it was convenient for us to choose the surface wires (the initial distribution) to be perfectly transmitting, so that any particle reaching the surface is lost from the system. We then selected a connectivity, K, and a disorder value for all the other wires in the lattice. The disorder within the wires was introduced by assuming that all the transmission occurs via tunnelling through a single eigenstate in each wire. This assumption was justified in [1] and allows us to make use of the Azbel distribution [19] for the transmission amplitude of disordered one-dimensional wires

$$P(|t|) = \frac{L_0}{L} \frac{1}{|t|} \qquad \exp(-L/L_0) \leqslant |t| \leqslant 1 \tag{23}$$

the disorder value being defined by the ratio L/L_0 (as is normal in these calculations, we also assume phase randomization across the wires). This expression is very simple and is thus not wasteful of computing time.

We can then commence the numerical recursive procedure: select K elements at random from the initial array and join these together to form a junction with reflection r' (stage 1 of figure 3). Next select a single one-dimensional wire and attach it to the junction to form a new, larger, Bethe lattice section with reflection r and transmission t (stages 2 and 3 of figure 3). Repeat the process N times, to form a new array of larger Bethe lattice sections. Once this new array has been constructed, discard the array of the previous generation and begin the entire process again. We can represent this procedure in the form of a flow chart, figure 4.

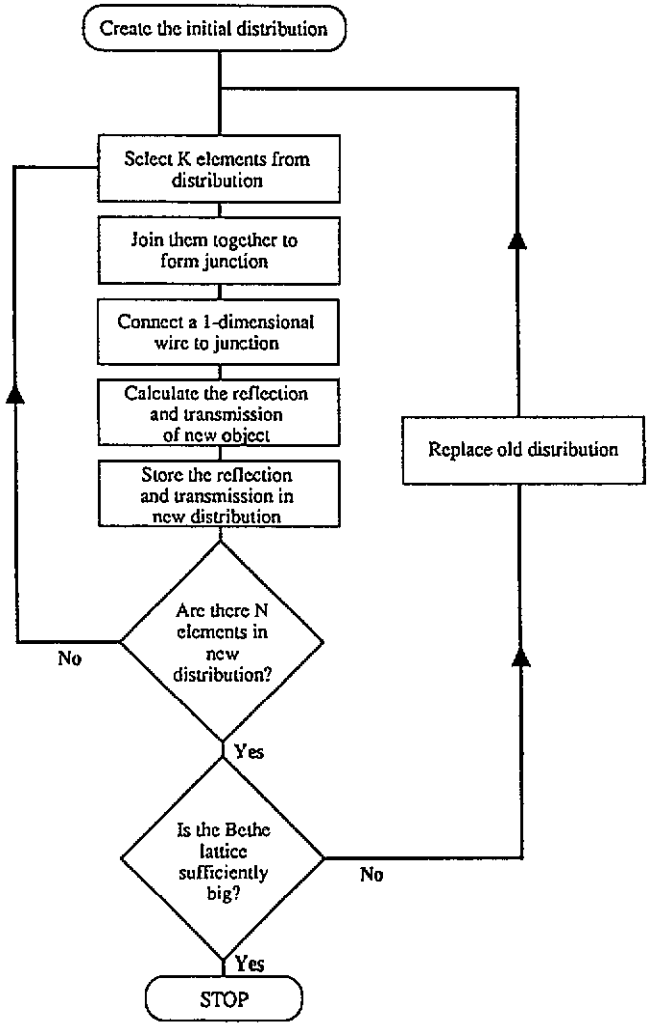

Figure 4. The algorithm used for carrying out the recursive calculation of the transmission probability distribution of a Bethe lattice.

4. Results and analysis

4.1. Behaviour of T with system size and disorder

We ran the simulations with array sizes of $N = 16\,384$ elements forming the distributions. For various disorder values, we calculated three different means: namely, the arithmetic mean $\log\langle T\rangle$, the geometric mean $\langle \log T\rangle$ and the harmonic mean $-\log\langle T^{-1}\rangle$, where $T = |t|^2$. In all cases we used a connectivity value of $K = 2$.

Figure 5 shows the behaviour of these quantities with increasing shell number, for three typical cases which we found. For all disorder values up to around 1.70, the means rapidly converge to some constant value, see figure 5(a). Above this value, the lines are noticeably more noisy and take longer to converge to a constant value. However, above a disorder value of 1.80 the means no longer converge to some constant value: the transmission probability decreases with increasing system size, figure 5(b). Quite clearly the lattice is in an insulating state, since the transmission probability extrapolates to zero at infinite shell number.

So, from the behaviour in these two regimes we predict that an Anderson metal–insulator transition must occur at a disorder value somewhere between 1.70 and 1.80. Figure 5(c) shows the typical behaviour of the means in this critical region; the data are extremely noisy. In particular, from disorders of 1.71 to 1.76 the transmissive behaviour is peculiar: it does not seem to settle into any regular type of behaviour. Nevertheless, for disorders below 1.76 we removed data for small shell numbers (where we knew the lattices had yet to reach their stable states) and used linear regression to fit straight lines through the remainder of the points. Using the intercept of the $\log T$ as an estimate of the average transmission probability, we plotted the graph shown in figure 6. According to MacKinnon [20], plotting the logarithm of each of the three calculated means against disorder should show that these quantities diverge from each other as the transition is approached from the metallic side. Figure 6 shows that this is indeed the case for our model. Near the transition the data points have large error bars, but we have not included these on the graph since the general trend of the curves is sufficient to emphasize the important behaviour.

4.2. The localization length

For high disorder we find that the transmission probability decreases with increasing shell number, figure 5(b). Clearly, in this regime a relationship of the form

$$\log T \propto -Cn \tag{24}$$

where C is a constant, n is the shell number and $\log T$ represents the appropriate mean. Now, we know that n represents a length scale on the Bethe lattice since it is the distance covered in travelling from the centre to any point on the lattice. Therefore in this regime, the transmission probability (and hence the conductance) decays exponentially and C must represent the inverse localization length.

We fitted a straight line through all graphs having the form shown in figure 5, for all disorders, and calculated the the negative of the inverse localization lengths. We plot these values against the disorder in figure 7. For low disorder the lattice is conducting and the localization length must be infinite, hence the inverse localization length must be zero. This is clearly seen in figure 7. At high disorder, the inverse localization length grows as the disorder increases in a more or less linear fashion. Between these regimes, the transition can be clearly identified, occurring at a disorder value near 1.70.

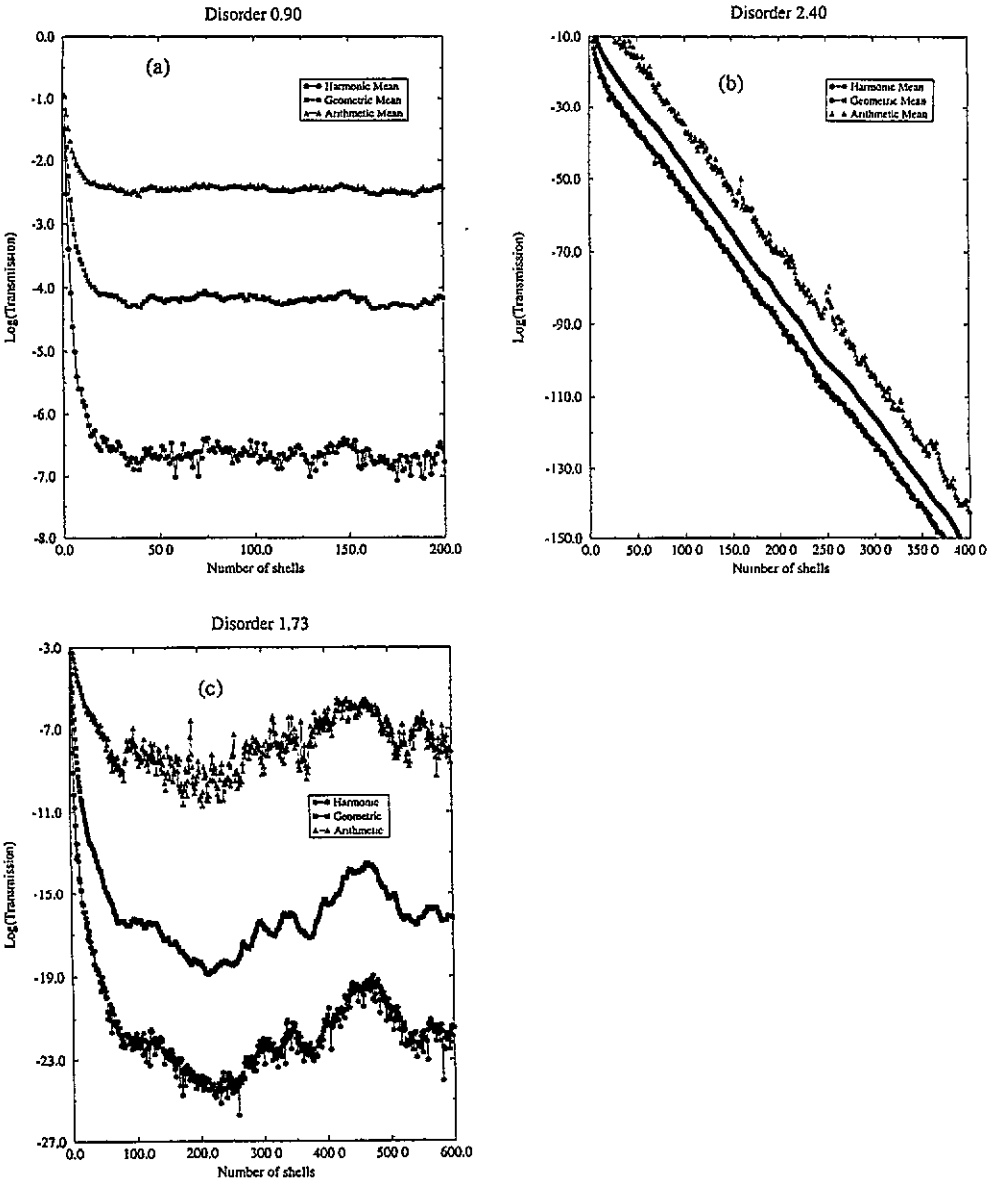

Figure 5. The logarithmic behaviour of the transmission for three distinct cases. In (a) the disorder is weak and the system quickly converges to a constant transmission. For the case of strong disorder (b), the transmission no longer reaches a constant value, but decreases exponentially. In graph (c) the data are extremely noisy and the infinite lattice behaviour is not easy to determine.

Unfortunately, the results of this simulation do not allow us to calculate a critical exponent for the transition. In a recent paper MacKinnon [5] confirmed that in order to obtain an accurate result for the exponent, it is essential that data must be taken very close to the transition point. The data obtained from our simulation are too noisy in this region, making any calculation of the exponent meaningless because of the large error which would be involved.

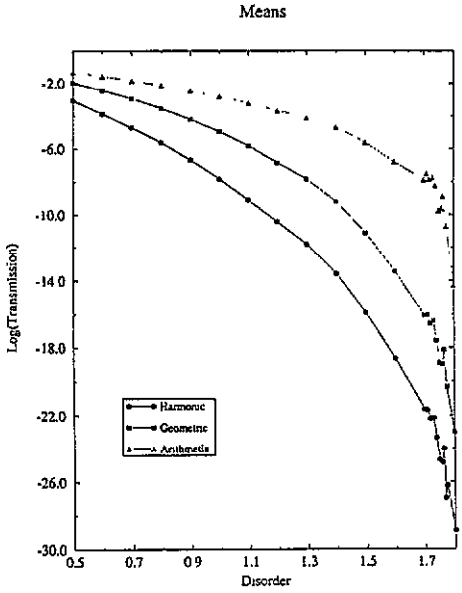

Figure 6. The logarithmic behaviour of the arithmetic, geometric and harmonic means of the transmission of the Bethe lattice with increasing disorder. Notice that they diverge from one another in the transition region.

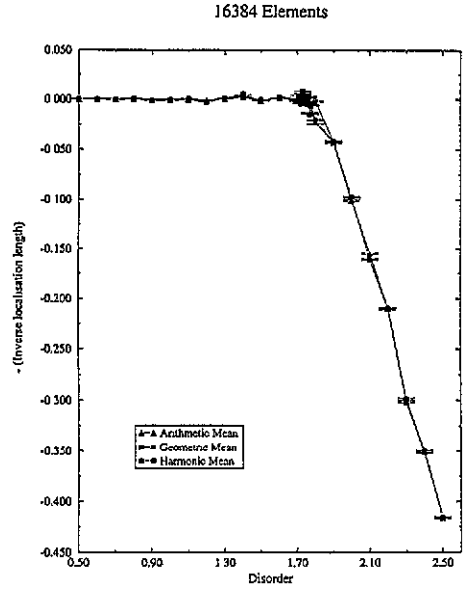

Figure 7. The inverse localization length is plotted against disorder, showing a transition to localized states at a disorder around 1.70–1.75.

There is no evidence in our simulation of a second transition, occurring between power-law and exponentially decaying states as predicted by Chalker and Siak [17]. However, this is due to the definition of our model: we make no distinction between the character of the states which carry the current. The precise form of the states which carry the current (which were shown to undergo a transition from power law to exponentially decaying by Chalker and Siak) are not of interest in this particular model. However, it is possible that this second transition does show up in our model through a change in the statistics of the conductance. However, the inevitable fluctuations near the metal–insulator transition are probably sufficient to mask this second transition, as is clear in the next section.

4.3. The conductance distribution

We now know from our analysis that the transition from metal to insulator in our model occurs at a disorder value near 1.70. This is the region where we want to study the conductance distribution in detail. However, it is useful to examine the distribution in the strong- and weak-disorder regimes also. In figure 8(a) we show the evolution of the distribution of $\log T$ with shell number for a disorder value of 1.30. The distributions were obtained by generating a histogram from the 16 384 array elements. The distribution maps onto itself as the lattice size increases.

In figure 8(b) the evolution of the $\log T$ distribution is shown for high disorder. In this regime, the distributions maintain their Gaussian shape as the shell number increases, but the entire distribution steadily shifts to smaller and smaller values of the transmission probability.

The behaviour of the distribution in the transition region is shown in figure 9. For disorder values from 1.71 to 1.74, the distributions for each shell number are only marginally

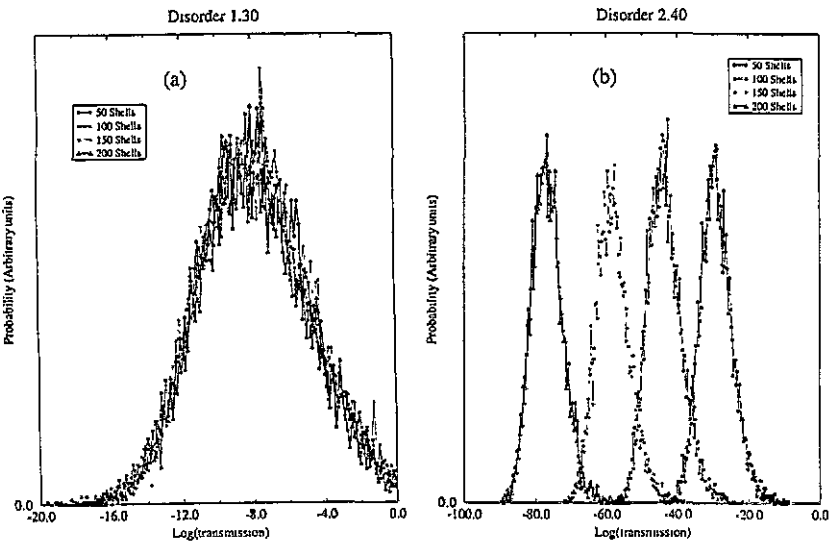

Figure 8. The behaviour of the $\log T$ distributions with shell number for strong and weak disorder. In (a) the disorder is weak and the distribution maps onto itself as the lattice size increases. In (b), however, the disorder is strong and the Gaussian distribution shifts with shell number to smaller and smaller values of transmission, while maintaining its shape.

shifted from one another and they are not shifted in any regular way. For example, the disorder value 1.72 shows most clearly that the distributions are slightly shifted from one another, but this shift is not systematic: the distribution for lattice size 600 shells is to the right of the distribution for 500 shells and the distribution for 400 shells is located closest to the origin. That is, they are shifted randomly (probably due to numerical fluctuations). But for disorder values above 1.75 the distributions begin to systematically shift to smaller values of transmission (corresponding to an increase in the lattice size, in contrast to the distributions for disorder 1.72) indicating that the transition has occurred somewhere between disorder values 1.74 and 1.75.

The most interesting feature of the distributions in this region is the form of their tails. There is little doubt that the tail on the RHS of the distributions (towards the origin) is longer than the tail on the LHS. This indicates that there exists a small, but significant, number of branches with transmission probability close to $T \sim 1$.

5. Discussion

Careful study of the distributions in the transition region indicates to us that the onset of insulating behaviour is signalled by the failure of the RHS tail of the $\log T$ distribution to reach the origin. Consider again figure 9. At disorder value 1.77, the tail of the distribution never reaches the origin and the distribution gradually shifts to the left as its size increases. However, for disorder value 1.74 the tail always reaches the origin and the distribution remains stationary with shell number.

Cohen *et al* [11] predict that distributions near the transition should be very broad. A numerical calculation of the resistance ρ of three-dimensional samples at the mobility edge

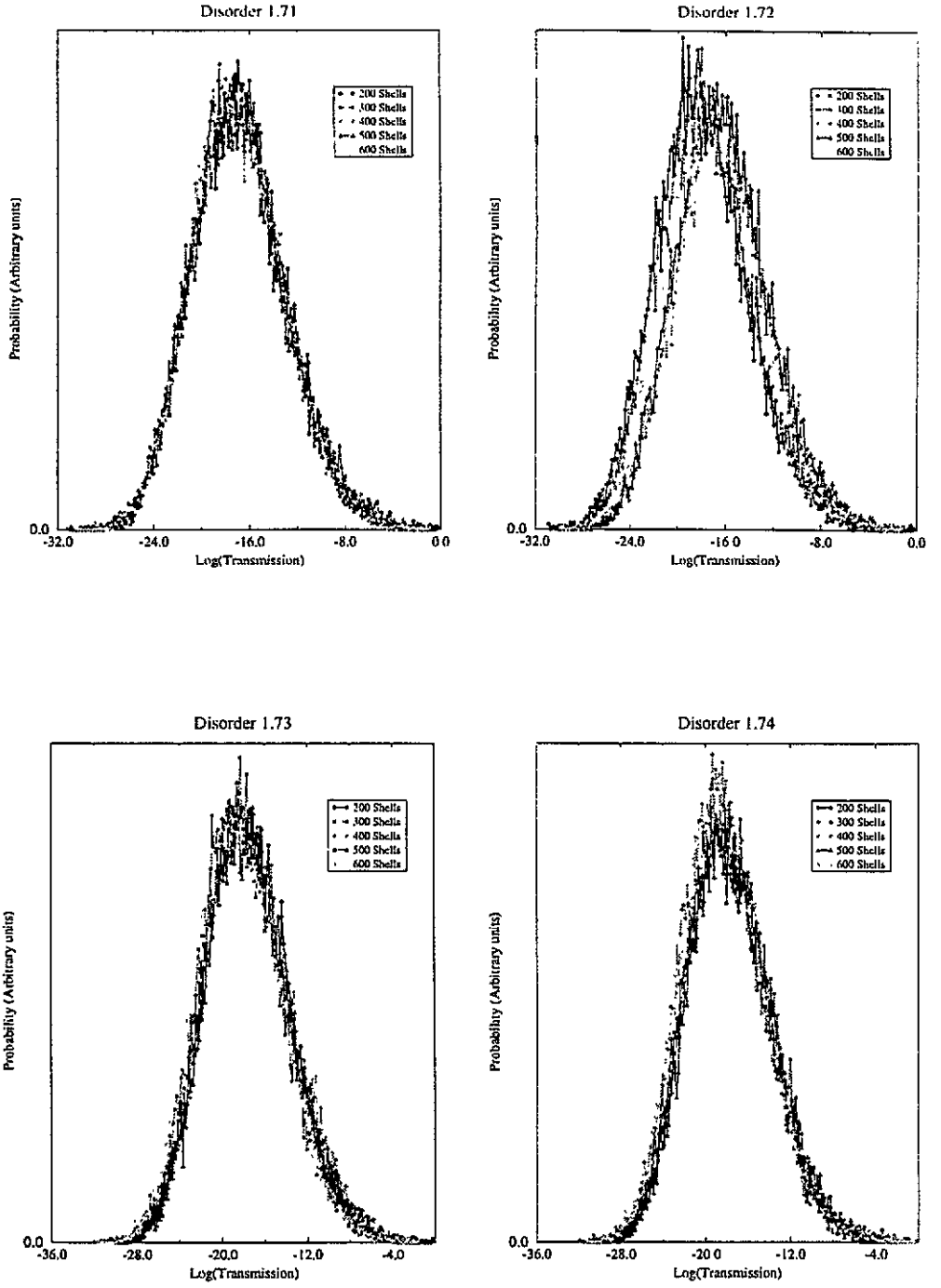

Figure 9. The behaviour of the $\log T$ distributions with shell number in the transition region. Notice the extended tails on the RHS and notice also that they fail to reach the origin when the disorder reaches 1.75.

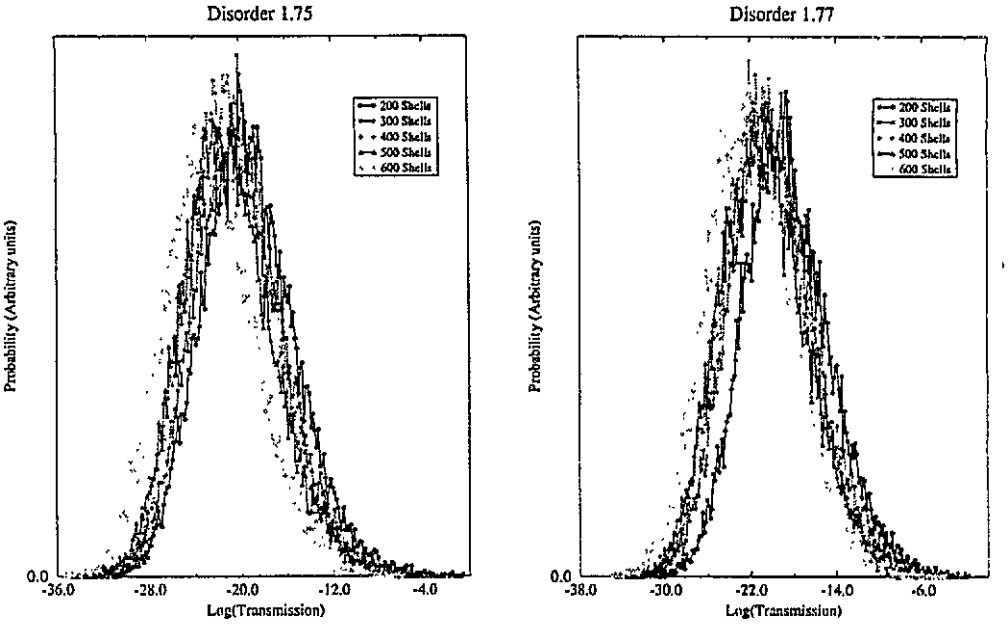

Figure 9. (Continued)

obtained a distribution of $\log \rho$ with a large tail towards high ρ. Markoš and Kramer [12] also calculated the $\log G$ distribution for small three-dimensional samples. They did not detect the long tail predicted by Cohen *et al*, but they were constrained by computational limitations and could not test large sample sizes. Our distributions do not exhibit tails as large as those predicted by Cohen *et al*; in fact the tails we find are much smaller. However, it is known that their method of calculation severely overestimates fluctuations, while our method is exact. But neither do we find distributions of the form found by Markoš and Kramer. Their distributions, in fact, resemble the distributions we find at weak disorder.

We must urge some caution on our results though. Both these other numerical studies were performed on 'real' three-dimensional lattices. Also, we know that our model does not reproduce certain features that we might expect to find in real lattices: namely, in the metallic regime of three-dimensional samples, the conductance distribution (as opposed to the logarithm of the conductance) should be Gaussian [12]. When we plot the conductance distribution we see only a peak around zero with a long tail towards high values. Changing the disorder merely changes the size of the peak and tail. Also, for one-dimensional systems the variance of the $\log G$ distributions is known to scale linearly with the mean for moderate disorder [7, 10, 21]. This behaviour is expected to hold in higher dimensions, but we see no evidence of it. In particular, 5(b) clearly shows that the variance remains constant no matter what value the mean takes.

6. Conclusion

We have studied the metal–insulator transition in detail on a Bethe lattice. In the transition region we found that the $\log T$ distributions were of Gaussian form, but had a long tail towards high values of transmission. For the Bethe lattice, the onset of localization seems to be signalled by a failure of this tail to reach the origin of $\log T$. Once the insulating

regime was reached, we found that the distributions maintained their Gaussian shapes with a long tail towards high T. Also, in this regime the distributions were found to move towards smaller values of T as the lattice was increased in size.

We have also shown that the distributions do not follow the predictions for regular lattices in the metallic regime and for moderately strong disorder.

Acknowledgments

PMB would like to thank Luis Martin-Moreno and John Roberts for helpful discussions. This work was supported in part by the European Union through science grant SCC*-CT90-0020. PMB would also like to thank the United Kingdom Science and Engineering Research Council for financial support.

References

[1] Bell P M and MacKinnon A 1993 *J. Phys.: Condens. Matter* **5** 8337
[2] Anderson P W 1958 *Phys. Rev.* **109** 1492
[3] Abrahams E, Anderson P W, Licciardello D C and Ramakrishnan T V 1979 *Phys. Rev. Lett.* **42** 673
[4] MacKinnon A 1990 *Proc. Int. Winter School on Localisation and Confinement of Electrons in Semiconductors (Mauterndorf, 1990)* ed F Kuchar *et al* (Heidelberg: Springer) p 111
[5] MacKinnon A 1994 *J. Phys.: Condens. Matter* **6** 2511
[6] Melnikov V I 1981 *Sov. Phys.–Solid State* **23** 444
[7] Pendry J B and Kirkman P D 1984 *J. Phys. C: Solid State Phys.* **17** 5707
[8] Slevin K M and Pendry J B 1990 *J. Phys.: Condens. Matter* **2** 2821
[9] Roberts P J 1992 *J. Phys.: Condens. Matter* **4** 7795
[10] Shapiro B 1987 *Phil. Mag.* B **56** 1031
[11] Cohen A, Roth Y and Shapiro B 1988 *Phys. Rev.* B **38** 12125
[12] Markoš P and Kramer B 1993 *Phil. Mag.* B **68** 357
[13] Bethe H H 1935 *Proc. R. Soc.* A **216** 45
[14] Abou-Chacra R, Anderson P W and Thouless D J 1973 *J. Phys. C: Solid State Phys.* **6** 1734
[15] Kunz H and Souillard B 1983 *J. Physique* **44** L411
[16] Shapiro B 1983 *Phys. Rev. Lett.* **50** 747
[17] Chalker J T and Siak S 1990 *J. Phys.: Condens. Matter* **2** 2671
[18] Landauer R 1992 *Phys. Scr.* T **1942** 110
[19] Azbel M Ya 1983 *Phys. Rev.* B **28** 4106
[20] MacKinnon A 1990 *Quantum Coherence in Mesoscopic Systems (NATO ASI Series B, vol 29)* ed B Kramer (New York: Plenum) p 415
[21] Anderson P W, Thouless D J, Abrahams E and Fisher D S 1980 *Phys. Rev.* B **22** 3519